IRANIAN JOURNAL OF CATALYSIS

Nitrogen doped TiO₂ for efficient visible light photocatalytic dye degradation

Jila Talat Mehrabad[a],*, Mohammad Partovi[b], Farzad Arjomandi Rad[a], Rana Khalilnezhad[c]

[a]Department of Chemistry, Bonab Branch, Islamic Azad University, Bonab, Iran.

[b]Department of Chemical, Faculty of Engineering, Tehran North Branch, Islamic Azad University, Tehran, Iran.

*[c]Department of Chemistry, Islamic Azad University Tehran North Branch, Tehran, Iran.*

ABSTRACT

In this study, Nitrogen doped TiO₂ photocatalysts were prepared by the sol gel method and physicochemical properties were characterized by X-ray diffraction (XRD), and scanning electron microscopy (SEM), photoluminescence, and energy dispersive X-ray spectroscopy (DRS) techniques. The XRD data indicated that the nanoparticles had the same crystals structures as the pure TiO₂. Photocatalytic properties of the nitrogen doped TiO₂ nanocatalyst and pure TiO₂ were compared for degradation of Blue 5 dye in visible light irradiation and the DRS results showed that the band gap of doped photocatalyst was smaller than that of the undoped TiO₂ and there was a shift in the absorption band toward the visible light region. The Photocatalytic properties of the nitrogen doped TiO₂ nanocatalyst were employed for degradation of crystal Blue 5 dye under visible light irradiation. The effects of pH, amount of photocatalysts, catalyst dosage, and dye concentration were also examined. The best results were reported for the concentration of 20 mg/L N-TiO₂ nano-particles. Also results showed that the photodecomposition of N-TiO₂ is complete at pH 11. Total organic carbon (TOC) analysis indicated 30 % mineralization of Blue 5 after 75 min irradiation.

*Keywords: Photocatalysis, Nanoparticles, Nitrogen doped TiO₂, Degradation, Blue 5 dye.*

1. Introduction

Today, the increasing volume of industrial waste containing organic pollutants has needed attempts to find new technologies for refining the polluted water [1]. In recent years, advanced oxidation processes (AOPs) are mostly used for the degradation of dyes and wastewater treatment [2-4]. The mechanism of AOPs process is based on the formation of a very reactive hydroxyl radical, which can oxidize a wide range of organic compounds. Among the various AOPs, heterogeneous photocatalysis has been widely used for photocatalytic degradation of organic pollutants from aqueous solutions. [5]. Compared to other metal oxide semiconductors (Fe₂O₃, CdS, ZnO, and WO₃, etc), titanium dioxide (TiO₂) is the most common material employed in the photocatalytic treatment of pollutants due to its high activity, good chemical inertness, non-toxicity and relatively inexpensive costs.

Moreover, TiO₂ presents a fairly high electron-hole recombination rate which is unfavorable to its photoactivity. Therefore, the defeat of recombination of photo-generated electron/hole pairs in the TiO₂ is important for improving the efficiency of photocatalytic activity [6]. The mechanism for the photocatalytic degradation of organic pollutants could be visualized as follows: when nano-TiO₂ is illuminated with ultraviolet (UV) light, electron is promoted from the valence band to the conduction band and this leads to the generation of a positive hole (h_{vb}^+) - electron (e_{cb}^-) pairs, according to Eq. (1):

$$TiO_2 + h\nu \longrightarrow e_{cb}^- + h_{vb}^+ \qquad (1)$$
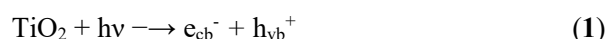
The positive hole can oxidize water and hydroxyl ions to produce the highly reactive hydroxyl radicals according to Eqs. (2) and (3):

$$h_{vb}^+ + H_2O \longrightarrow {}^\bullet OH + H^+ \qquad (2)$$
$$h_{vb}^+ + OH^- \longrightarrow {}^\bullet OH \qquad (3)$$
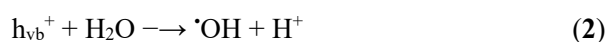
Alternatively, the electron in the conduction band is trapped by an electron acceptor such as oxygen to

*Corresponding author.

E-mail address: jila.talat96@gmail.com (J. Talat Mehrabad)

produce superoxide radical anion ($O_2^{\bullet -}$) according to Eq. (4):

$$e_{cb}^- + O_2 \longrightarrow {}^{\bullet -}O_2 \tag{4}$$

The hydroxyl radicals are powerful oxidants with the oxidation potential of 2.8 V (NHE), they can be used to oxidize most organic contaminants. However, TiO_2 has a large band gap (3.20 eV for anatase TiO_2) and therefore, restricts the applicability of TiO_2 as a photocatalyst [7]. Two main factors which manage the photocatalytic activity of TiO_2 at first are: lowering band gap energy in visible region and inhibition of electron hole recombination rate. Doping is one of the techniques to overcome such limitation. This can decrease the band gap energy and, as a result, shift the absorption band to the visible range [8,9]. For increasing photocatalytic activity many attempts have been developed to sensitize modified TiO_2, such as doping with transition metals, nonmetal atoms and organic materials. Replacement of non-metallic elements, such as C [10], N [11], S [12], I [13] and P [14], seems to be a very favorable way to improving optical property of TiO_2. Especially, the synthesis of N-doped TiO_2 (N-TiO_2) has been the subject of recent photocatalyst researches [15]. The various methods used for doping of TiO_2 involve physical methods (mechanical milling [16], magnetron sputtering, etc.). However, physical methods often need expensive devices [17], and chemical methods always contain a high temperature in the preparation method [18]. The sol–gel process is certainly the simplest and the cheapest one and also it is an attractive method for low temperature synthesis of N/TiO_2.

In this work, we report the photocatalytic degradation of Blue 5 dye using a recently developed class of TiO_2 nanoparticles doped with nitrogen at the low temperature. We successfully prepared N-TiO_2 particles by the sol gel method. The results indicated that N-TiO_2 nanoparticles synthesized in this way showed a considerably enhanced activity of photodecomposition of organic pollutants. The structural properties of the prepared catalysts were characterized using X-ray diffraction (XRD), scanning electron microscopy (SEM), photoluminescence (PL), UV–Vis diffuse reflectance spectroscopy (DRS).

2. Experimental

2.1. Materials

Titanium tetraisopropoxide (Ti(OC$_3$H$_7$)$_4$) was used as the titania precursor. All compounds such as ethanol (95%), aqueous ammonia solution (28%) and nitric acid were obtained from Merck (Germany).

2.2. Dye

The reactive Blue 5 dye (λ_{max}= 597 nm) that was used in this paper was obtained from Sigma-Aldrich. The chemical structure of this dye is shown in Fig. 1.

2.3. Light sources and photoreactors

The reactor used was the batch type with one-liter capacity and the visible light source was a 500 W halogen lamp (Osram).

2.4. Preparation of the N/TiO₂ catalyst

The nitrogen-doped titania nano catalysts were prepared by a sol–gel method. The sol solution was prepared by adding 10 ml of Ti [OCH (CH$_3$)$_2$]$_4$ (Aldrich, 97%) to 40 ml ethanol and 10 ml aqueous ammonia solution (28%wt) and 2ml HNO$_3$. The mixture was vigorously stirred using a magnetic stirrer during addition and was maintained for a further 2 h after addition of the precursor at room temperature. Then a colloidal solution of TiO_2 nano crystals was formed. Finally, a gray powder was obtained after centrifugation and the sol was aged for 6 h. The dried solid was calcinated at 400 °C for 4 h in a furnace, the light yellow powder was obtained. Pure TiO_2 nano crystals were prepared with the same procedure without addition of ammonia during the hydrolysis of the titanium precursor.

2.5. Characterization

XRD patterns for phase identification and crystallite size calculation were recorded with a Siemens D5000 XRD, using Cu–Kα radiation (recorded in the $2\theta = 20–70°$). The average crystallite size (d in nm) was calculated by Scherrer's equation Eq. (5):

$$d = \frac{k\lambda}{\beta \cos \theta} \tag{5}$$

Where k is a constant equal to 0.89, λ is the X-ray wavelength equal to 0.154056 nm, β is the full width at half maximum intensity, and θ is the half diffraction angle [19].
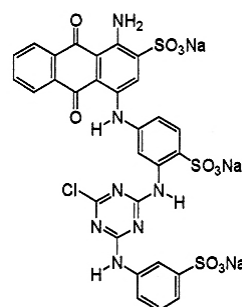

Fig. 1. Chemical structure and properties reactive Blue 5 (C$_{29}$H$_{17}$ClN$_7$Na$_3$O$_{11}$S$_3$).

SEM analysis was performed on Au-coated samples using a Philips apparatus model XL30.

Total organic carbon (TOC) measurements were carried out by the TOC analyzer (Shimadzu TOC-Vcsn).

The DRS of the samples was obtained using Avaspec-2048 TEC spectrometer to determine the optical band gap (E_g) of the catalysts. The band gap energies of all samples were calculated by the Eq. (6):

$$E_g \text{ (ev)} = 1240/ \lambda \text{ (nm)} \qquad (6)$$

Photoluminescence emission spectra of the samples were recorded using a JASCO luminescence spectrometer with the excitation wavelength of 320 nm.

2.6. Photocatalytic Activity Determination

Photocatalytic activities of the prepared nitrogen doped TiO_2 photocatalyst was evaluated by the degradation of Blue 5 dye under visible light. For all photocatalytic experiments, a batch reactor was used, it was filled with 100 ml of aqueous suspension of Blue 5 (20 mg/L) of photocatalysts. A visible lamp was used as the light source. Prior to irradiation, the suspension was magnetically stirred in the dark for approximately 30 min to ensure the establishment of an adsorption/desorption equilibrium among the photocatalyst particles and dye. During the course of visible light irradiation, a suspension of about 5mL was taken out after regular intervals, centrifuged, and then filtered through a millipore filter. The filtrates were then studied by UV–vis spectroscopy.

3. Results and Discussion

3.1. Characterization of photocatalysts

Fig. 2 shows XRD patterns of N-TiO₂ calcined at 400 ℃. The XRD patterns in the range of 2θ diffraction angle between 20 and 80° were made to obtain the crystallite size and phase composition of nanoparticles.

The XRD pattern shown in Fig. 2 mainly consists of an anatase with a minor rutile phase (80: 20), indicating that the N dopant in TiO_2 did not influence the crystal patterns of TiO_2 particle [20]. The photocatalyst shows the dominant anatase phase peaks at 2θ = 25.2(101), 38(004), 48.2(200), and 62.5°(2004) and the small fraction of the rutile phase with peaks at 2θ = 27.5(110), and 54°. The average crystalline size is calculated according to the Debey-Scherres equation is about 18 nm [21].

Fig. 3 shows SEM images of nitrogen doped TiO_2 nanoparticles. This image exhibits the particles with a spherical morphology and a dense structure with good homogeneity and is to some extent agglomerated. There is an uneven distribution of agglomerated particles. The SEM micrographs of the sample show that the amounts of Ndoped TiO_2 did not influence the morphology of the sample.

Fig. 4 shows the optical absorption of nano TiO_2 and N-doped TiO_2 nanoparticles. The absorption wavelength for N-doped TiO_2 significantly has a red shift from TiO_2 due to the electronic transition between the defect level and the band structures of TiO_2. The band gap energies of all samples are presented in Table 1. The results indicated that N-doped TiO_2 decreased the optical bandgap energy, whereas a decrease in the E_g value for N-TiO_2 is greater than that of the pure TiO_2. Fig. 5 shows this large reduction of band gap may be attributed to the doping of N as impurities into the surface TiO_2 shifting away from the center of the band gap toward the VB [22].

Fig. 6 shows the PL spectra of the pure TiO_2 and N-doped TiO_2 nanoparticles excited by 320 nm. The PL emission spectra can be used to release the efficiency of charge carrier trapping, immigration, transfer and to know the fate of photo-induced electrons and holes in the semiconductor.
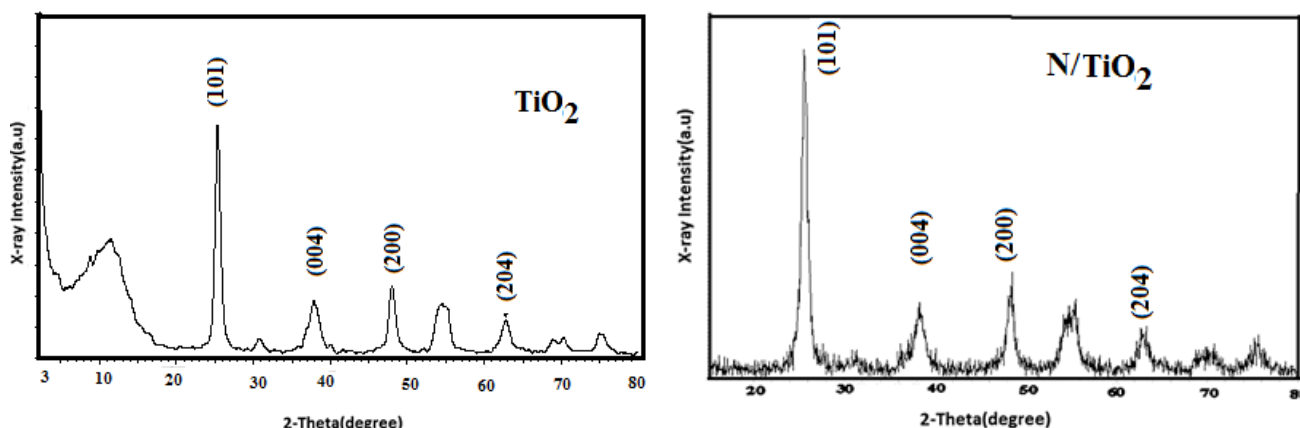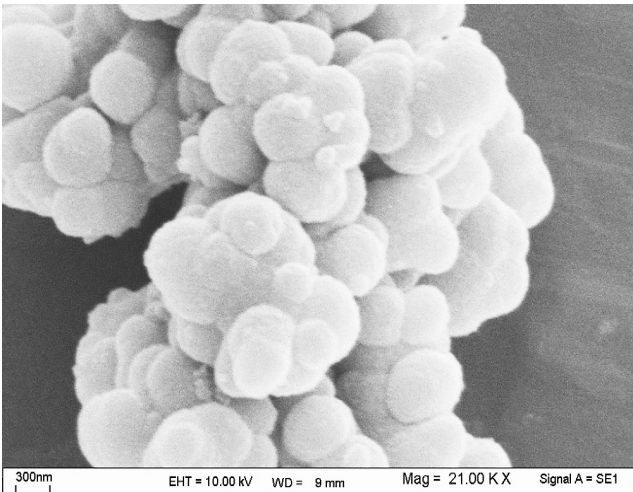

Fig. 2. XRD patterns of TiO₂ and N-TiO₂.

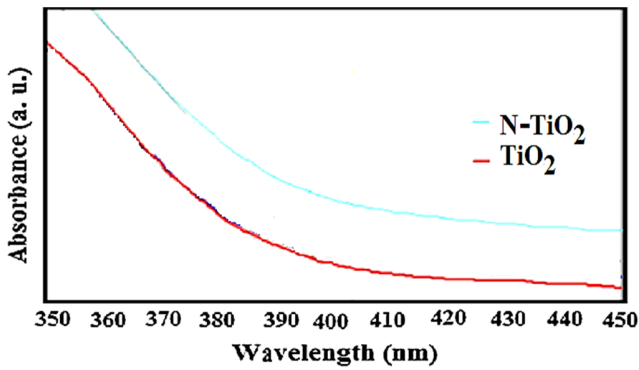**Fig. 3.** SEM images of prepared nitrogen doped TiO$_2$ nanoparticle.

Fig. 4. The DRS-UV-Vis spectra of TiO$_2$ and N/TiO$_2$ nanoparticles.

Table 1. E$_g$ values for TiO$_2$ and N/TiO$_2$ nanoparticles.

Catalyst	λ_{max} (nm)	E$_g$ (eV)
TiO$_2$	392	3.61
N/TiO$_2$	404	3.07
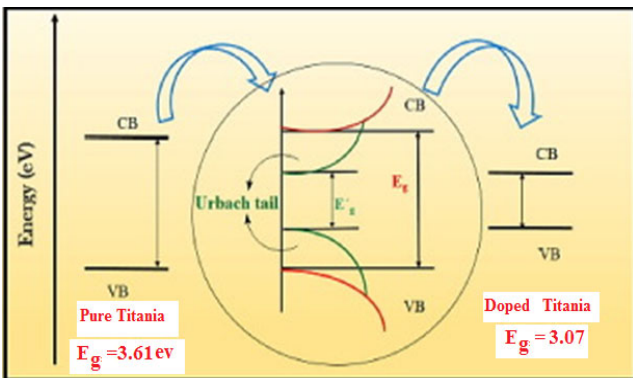
Fig. 5. E$_g$ comparison of TiO$_2$ and N/TiO$_2$ nanoparticles.
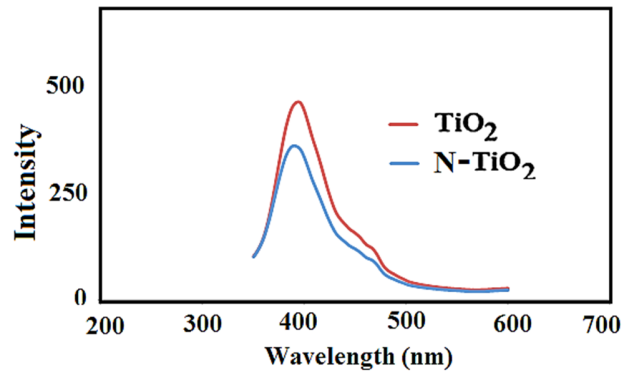

Fig. 6. PL spectra of pure TiO$_2$, N/TiO$_2$.

The lower intensity of the peak recommends that the N-doped on the surface of TiO$_2$ could effectively prevent the recombination probability of photo-generated electrons and holes, and therefore the catalytic activity decreased [23]. These results show that the photodegradation of N-TiO$_2$ is better than TiO$_2$.

3.2. Photocatalytic Activity

Fig. 7 shows the efficiency of photo degradation (X) of the nitrogen doped TiO$_2$ for the removal of Blue 5 as a function of time at λ = 597 nm. The batch experiments were carried out with 100 mL dye solutions. Dye solutions were stirred after adding 0.08 to 0.2 mg/L catalyst with 20 ppm dye concentration. According to the results, the optimum N-TiO$_2$ catalyst was 0.16 mg/L because of the small difference between catalytic amounts (0.14 and 0.16) and economic issues, the optimum N-TiO$_2$ catalyst amount has been determined to be 0.14 mg/L. Therefore, the progress of photo catalytic degradation was monitored by measuring the absorbance of the solution samples by UV-Vis spectrophotometer at λ_{max} = 597 nm. The percentage of degradation was calculated using the Eq. (6):

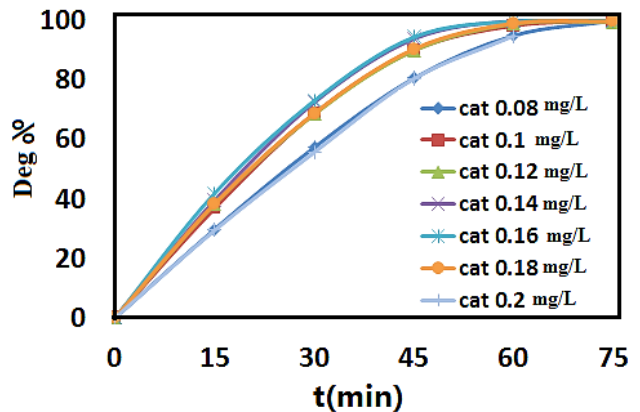$$Degradation\ (\%) = \frac{c_0 - c}{c_0} \times 100 \qquad (6)$$

Fig. 7. The efficiency of N-TiO$_2$ for the removal of Blue 5 as a function of time at λ = 597 nm.

Where C_0 is the initial dye concentration and C is the dye concentration after the treatments. As shown in Fig. 4, nitrogen doped TiO$_2$ has a high efficiency of 99.5% in crystal Blue 5 decolorization in 75 minutes with 0.18 mg/L of the catalyst.

3.3. Effect of pH on the photocatalytic activity of N-TiO$_2$

To investigate the effect of pH on reactive Blue 5 structure, the dye solution with the concentration of 20 mg/L at different pHs were prepared. As shown in Fig. 8, the reactive Blue 5 is stable at pH within the range of 2 to 12.

Normally, pH value affected the photocatalytic activity of N-TiO$_2$ nanoparticle. Fig. 9 shows the efficiency of pH for the degradation of Blue 5 as a function of time. For exploring the effect of pH, the solution's pH was initially adapted by adding 0.01N NaOH or 0.01N H$_2$SO$_4$ and by controlling with a pH meter. Zero-point charge pH (pHpzc) of the catalyst was estimated at 6.5 as shown in the inset of the figure. At pH$_{pzc}$, the catalyst surface has a net neutral charge. At pH 2, the neutral catalyst surface cannot absorb sufficient neutral Blue 5 molecules and hence its degradation amount quickly decreases. It can be seen that the photo degradation of N-TiO$_2$ is complete at pH 11 [24].

3.4. Effect of dye concentration

The effect of the initial dye concentration on the rate of degradation was studied by varying the initial concentration over a range of 20-40 ppm at 0.1 mg/L N-TiO$_2$ catalyst. Fig. 10 shows the effects of the initial reactive Blue 5 concentration on photo catalytic degradation efficiency.

It can be observed that as the dye concentration increases, decolorization declines. This may be attributed to; when the dye concentration increases, the number of dye molecules adsorbed is increased on the
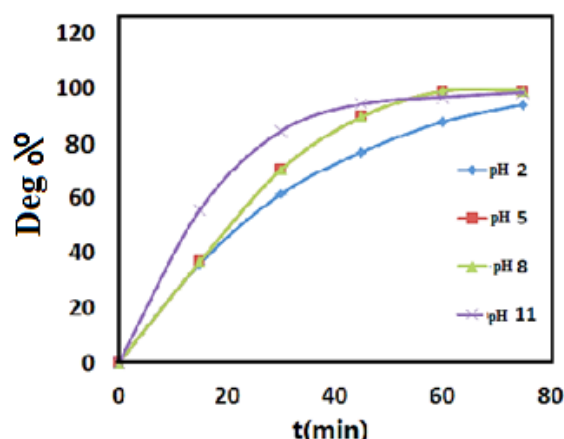

Fig. 9. Effect of pH on dye degradation.

catalyst surface and therefore less light can reach the catalyst surface. On the other hand, when the dye concentration increases, the increasing light scattering can decrease photocatalytic removal of Blue 5 due to the decrease of light penetration.

3.5. Effect of catalyst dosage

The apparent reaction rate constants (k_{ap}) for the photocatalytic removal of Blue 5 were obtained from the slope of the semi-logarithmic graphs. A series of experiments were conducted to study the effect of catalyst dosage on the degradation of Blue 5 and to get the optimum catalyst loading by varying the nano doped TiO$_2$ from 200 to 600 mg L^{-1} in 100 mL Blue 5 solution of 20 ppm concentration. Fig. 11 shows the variations of pseudo first order rate constants with four different catalyst dosages under visible light. The rate of degradation improved with the increase of catalyst loading up to 400 mg L^{-1} and a decrease was observed when catalyst dosage increased from 400 mg L^{-1}. increasing N-doped TiO$_2$ dosage resulted in the increase of the number of photons absorbed and the number of dye molecules adsorbed with respect to an increase in the number of catalyst molecules until the active surface becomes constant.
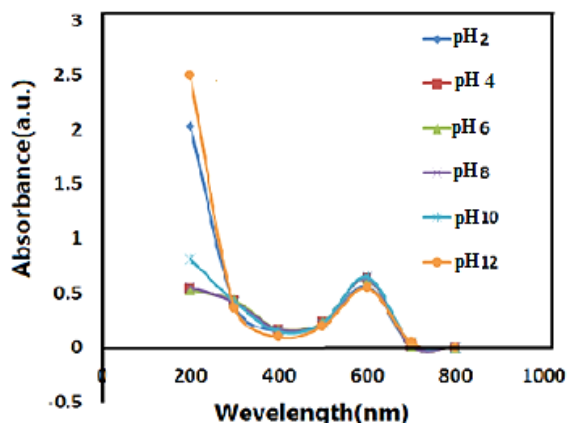

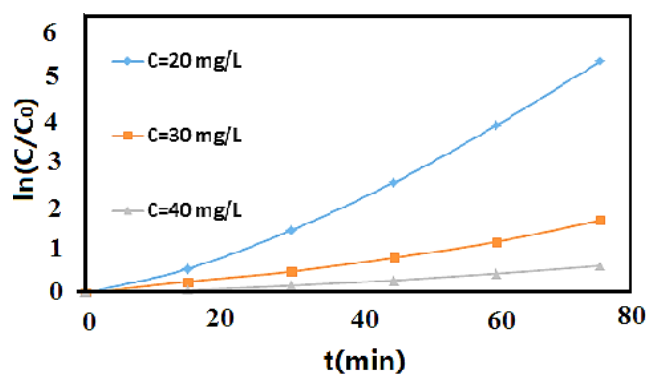**Fig. 8.** Effect of pH on the photocatalytic activity of N-TiO$_2$.

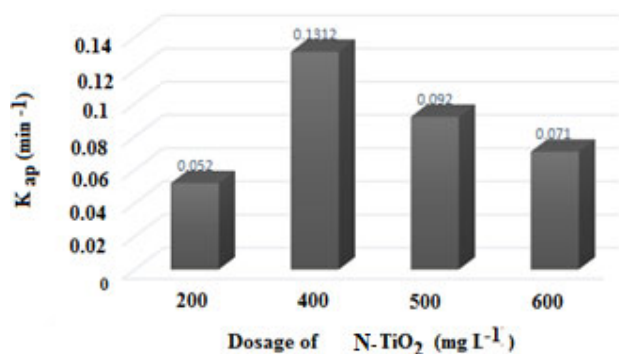**Fig. 10.** Effects of dye concentrations in dye degradation.

Fig. 11. Effects of various dosages of N-TiO$_2$ nanoparticles on the degradation of Blue 5.

In the case of the catalyst overdose, due to decreasing light penetration, the increase of light scattering decreases photocatalytic removal of Blue 5 [26].

3.6. Total organic carbon analysis

Total organic carbon (TOC) values are related to the total concentration of organics in the solution an organic compound and are often used as a non-specific indicator of water quality. One of the important advantages of AOP comparing to the other treatment methods is that AOP can mineralize the pollutants. As the UV-Vis spectrophotometer only shows how much dye is eliminated and it does not show how much organic pollutants exist in the water, it is necessary to analyze the TOC of samples to measure the extent of mineralization, which is an important factor and shows the efficiency of photocatalysts [23]. The kinetics of total organic carbon (TOC) disappearance was examined for the NCs at Fig. 12. It shows that about 10% of the TOC was degraded during the 30 minutes and more noticeably during the one hour of the reaction with over 22% of TOC reduction. About 30% of carbon disappeared after 75 minutes of visible irradiation.
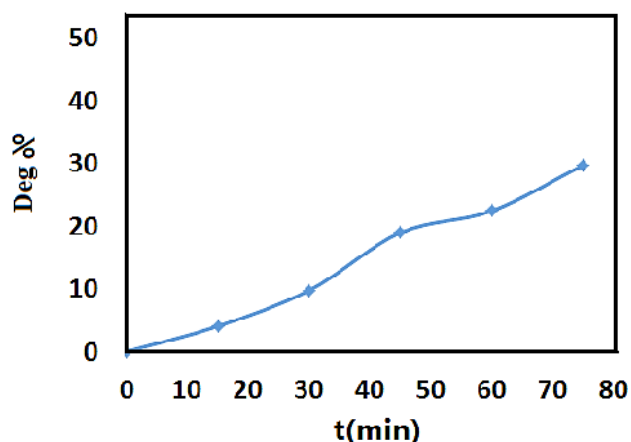

Fig. 12. The amount of TOC.

4. Conclusions

Nitrogen doped TiO$_2$ powder was synthesized by the sol gel method. It was found that N-TiO$_2$ showed significantly higher photocatalytic activity on the degradation of Blue 5 under visible light irradiation. The XRD patterns indicated that adding nitrogen to TiO$_2$ could prevent the phase transformation from anatase to rutile. DRS results indicated a considerable decrease in the Eg value for N/TiO$_2$ nanoparticles in comparison with bare TiO$_2$ nanoparticles. This is mainly due to the high dispersion of the nitrogen onto TiO$_2$ surface. The best results of dye degradation were reported in the concentration of 20 ppm N-TiO$_2$ nanoparticles. Results showed that the photodecomposition of N-TiO$_2$ is complete at pH 11.

References

[1] I. Oller, W. Gernjak, M.I. Maldonado, L.A. Perez-Estrada, J.A. Sanchez-Perez, S. Malato, J. Hazard. Mater. 138 (2006) 507–517.
[2] J. Yu, H. Yu, C.H. Ao, S.C. Lee, J.C. Yu, W. Ho, Thin Solid Films 496 (2006) 273–280.
[3] A. Nezamzadeh-Ejhieh, Z. Ghanbari-Mobarakeh, J. Ind. Eng. Chem. 21 (2015) 668–676.
[4] E. Hapeshi, A. Achilleos, M.I. Vasquez, C. Michael, N.P. Xekoukoulotakis, D. Mantzavinos, D. Kassinos, Water Res. 44 (2010) 1737- 1746.
[5] A. Fujishima, X. Zhang, D.A. Tryk, Surf. Sci. 63 (2008) 515–582.
[6] B. Khodadadi, Iran. J. Catal. 6 (2016) 305-311.
[7] O. Legrini, E. Oliveros, A.M. Braun, Chem. Rev. 93 (1993) 671-698.
[8] A. Ramazania, S. Taghavi Fardooda, Z. Hosseinzadeha, F. Sadrib, S.Woo Jooc, Iran. J. Catal. 7 (2017) 181-185.
[9] U.G. Akpan, B.H. Hameed, J. Appl. Catal. A 375 (2010) 1–11.
[10] Y. Park, W. Kim, H. Park, T. Tachikawa, T. Majima, W. Choi, Appl. Catal. B 91 (2009) 355-361.
[11] E. Finazzi, C.D. Valentin, A. Selloni, G. Pacchioni, J. Phys. Chem. A 111 (2007) 9275–9282.
[12] F. Tian, C. Liu, J. Phys. Chem. B 110 (2006) 17866–17871.
[13] Q. Zhang, Y. Li, E.A. Ackerman, M. Gajdardziska-Josifovska, H. Li, Appl. Catal. A 400 (2011) 195-202.
[14] K.S. Yang, Y. Dai, B.B. Huang, J. Phys. Chem. C 111 (2007)18985–18994.
[15] A.T. Kuvarega, R.W.M. Krause, B.B. Mamba, J. Phys. Chem. C (2011) 22110-22120.
[16] B. Liu, S. Yin, R. Li, Y. Wang, T. Sato, J. Ceram. Soc. Jpn. 115 (2007) 692–696.
[17] R. Asahi, T. Morikawa, T. Ohwaki, Y. Taga, K. Aoki, Sci. Total Environ. 293 (2001) 269–271.
[18] S. Livraghi, M.R. Chierotti, E. Giamello, G. Magnacca, M.C. Paganini, G. Cappelletti, C.L. Bianchi, J. Phys. Chem. C 112 (2008) 17244–17252.

[19] A.L. Patterson, J. Phys. Rev. 56 (1939) 978–982.

[20] Y. Li, S. Peng, F. Jiang, G. Lu, S. Li, J. Serb. Chem. Soc. 72 (2007) 393-402.

[21] S. Aghabeygi, R. Kia Kojoori, H. Vakili Azad, Iran. J. Catal. 6 (2016) 275-279.

[22] H.R. Pouretedal, M. Fallahgar, F. Sotoudeh Pourhasan, M. Nasiri, Iran. J. Catal. 7 (2017) 317-326.

[23] J. Talat-Mehrabad, M. Khosravi, N. Modirshahla, M.A. Behnajady, Desalin. Water Treat. 57 (2016) 10451-10461.

[24] F. Soori, A. Nezamzadeh-Ejhieh, J. Mol. Liq. 255 (2018) 250–256.

[25] I.K. Konstantinou, T.A. Albanis, J. Appl. Catal. B 49 (2004)1–14.

[26] C.C. Wong, W. Chu, Chemosphere 50 (2003) 981–987.